Integration of bright color centers into arrays of silicon carbide nanopillars

Enora Vuillermet, N. Bercu, S. Kochtcheev, M. Lazar

Integration of bright color centers into arrays of silicon carbide nanopillars

E. Vuillermet,[1] N. Bercu,[2] S. Kostcheev,[1] and M. Lazar[1]
[1)]*Light nanomaterials, nanotechnologies laboratory, CNRS UMR 7076, University of Technology of Troyes, Troyes, France*
[2)]*Light nanomaterials, nanotechnologies laboratory, CNRS UMR 7076, University Reims Champagne-Ardenne, Reims, France*

(*Electronic mail: enora.vuillermet@utt.fr)

(Dated: 2 July 2025)

Silicon carbide (SiC) is a wide-bandgap semiconductor combining mature fabrication processes with the ability to host optically active point defects, called color centers, making it ideal for quantum technologies. This study focuses on silicon vacancy defects in 4H-SiC, integrated into nanopillar arrays fabricated via ion implantation, e-beam lithography, and reactive ion etching. SiC nanopillars with a height of 1.4µm are formed and arrays with varying pillar diameters and spacings are obtained. Cathodoluminescence measurements at 80 K reveal a 2–4 times improvement in light collection efficiency from the defects compared to unstructured SiC. The cathodoluminescence intensity increases with a smaller pillar spacing and a larger diameter. These findings demonstrate the potential of SiC nanopillar arrays as scalable platforms for enhancing quantum photonic device performance.

Silicon carbide (SiC) is a wide-bandgap semiconductor that has been used for decades in power device applications[1]. The maturity of its fabrication processes has resulted in the commercialization of high-quality wafers with minimal defects[2], enabling the controlled integration of point defects within the material. This has recently driven the development of SiC as a host for bright color centers with long spin coherence times for quantum applications[3,4]. Compared to other materials, such as diamond and rare-earth-doped semiconductors, silicon carbide offers significant advantages for quantum device fabrication due to its well-established processes, including epitaxial growth[5], doping (n and p-type)[6], and etching[7]. These make SiC an ideal candidate for developing quantum platforms and devices[8,9], such as magnetic field sensors[10], quantum computing systems[11], and single-photon sources (SPSs) integrated into electronic or CMOS devices[12]. However, due to the high refractive index of SiC compared to air (around 2.6)[13], light emitted from the color centers is predominantly reflected at the SiC/air interface, leading to the need for devices that isolate single-photon sources while increasing the collection efficiency of the emitted photons.

Previous studies have demonstrated that integrating color centers into dielectric photonic crystal (PC) structures, such as microdisks[14], optical cavities[15], or nanopillars[16], can achieve strong light confinement and enhanced light-matter interaction at the sub-micron scale[17]. In the case of nanopillars, the guided resonant modes within the high-indexed structures can be coupled with the embedded single photon emitters, leading to an enhanced spontaneous emission rate of the point defects. Optical simulations from previous studies[18,19] indicate that the strong coupling between the pillar modes and the color centers increases the fraction of emitted light that escapes into free space from the top of the SiC pillar. In that case, nanopillars improve light extraction compared to bulk SiC, where most light gets reflected back into the substrate.

In this work, we focus on the single silicon vacancy defect (V_{Si}) in 4H-SiC, a promising quantum defect with electronic spin states that can be manipulated at room temperature (RT), exhibiting spin coherence times of approximately 100µs at RT[20] and up to 20ms at cryogenic temperatures[21]. Ion implantation is used to generate the color centers into n^+-doped 4H-SiC substrates. The implanted samples are then etched to form the different nanopillar arrays. This study completes the experimental works of S. Castelletto *et al.*[22] and M. Radulaski *et al.*[16] and ensures that the silicon vacancies are generated exclusively within the nanopillars, avoiding defect formation in the substrate between the photonic structures. We also investigate the effects of nanopillar array periodicity on light collection efficiency. The pillar spacings were chosen based on the theoretical work realized by Ahamad *et al.*[18], which predict that for specific arrays periodicity, the coherent superposition of the electric and magnetic dipolar and quadrupolar Mie scattering moments of SiC nanopillars enhances the spontaneous emission of the V_{Si} centers. Using cathodoluminescence (CL) at 80 K, we demonstrate a 2-4 times improvement in light collection from silicon vacancies compared to an un-

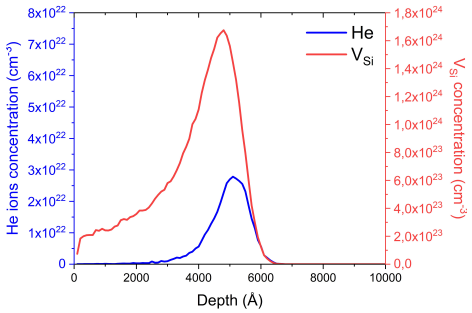

FIG. 1. SRIM-TRIM simulations depth profiles of the helium ions introduced and silicon vacancies generated during ion implantation.

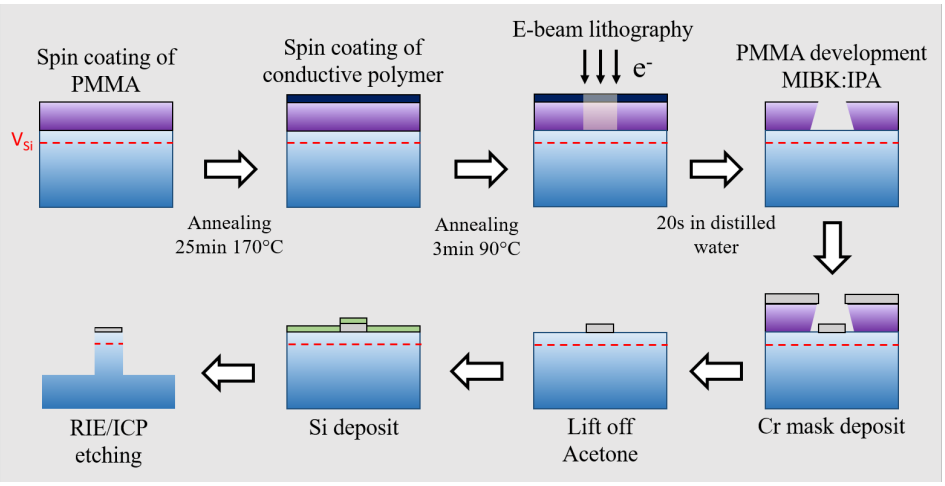

FIG. 2. Fabrication steps of the 4H-SiC nanopillars.

structured SiC substrate. These results highlight the potential of SiC nanopillar arrays as a scalable platform for quantum photonic applications.

The samples used in this study are commercial 4° off-axis n^+-doped (1×10^{18}cm^{-3}) 4H-SiC substrates from SiCrystal GmbH. They were implanted with helium ions at an energy of 120keV and a dose of 4×10^{17}cm^{-2} to form the V_{Si} defects. SRIM-TRIM simulations[23,24] indicate that the silicon vacancies are primarily generated at a depth of 480nm from the Si face of SiC (FIG.1). After ion implantation, one sample is kept as a reference, while the other one is processed to form the nanopillar arrays. For the latter, electron beam (e-beam) lithography is performed using a Raith e-line scanning electron microscope (SEM) operating at 20keV with an aperture of 30µm and an exposure dose of 200µC/cm^2. For this step, a 450 nm-thick PMMA resist is used to pattern the samples and is developed, after e-beam exposure, into a solution of MIBK:IPA for 1min20s. Following this, a 150nm-thick chromium hard mask is deposited via electron beam evaporation at a deposition rate of 0.1nm/s using the MEB400 system from Plassys. Lift off of the mask occurs in a solution of acetone under agitation. Reactive ion etching with inductively coupled plasma (RIE/ICP) is then carried out in a MU400 system of Plassys to form the SiC pillars. The plasma is generated at low pressure (1.067Pa) using a gas mixture of 10sccm SF_6 and 2sccm O_2 (the unit "sccm" stands for Standard Cubic Centimeters per Minute), with 100W of RIE power and 1000W of ICP power. An etching rate of 4.7nm/s is thus achieved under a bias of -156V. To avoid micro-masking, a phenomenon where small particles or residues act as unintended masks, leading to non-uniform etching and the formation of rough uneven surfaces[25,26], a 100nm-thick silicon layer is deposited on the samples before SiC etching. After the etching of the pillars, the remaining chromium mask is removed using a chromium etchant solution. The plasma etching parameters were optimized through multiple experiments designed to etch SiC power devices[27]. Fabrication steps of the 4H-SiC nanopillar arrays are summarized in FIG.2. Further details are included in the Supplementary Materials of this paper.

The resulting SiC nanopillars (FIG.3) have a height of 1.4µm, with diameters ranging from 350 to 700nm. We chose these dimensions according to the results of previous studies[16,18,19,22] (see Supplementary Materials). The arrays have an area of 100×100µm^2, with different pillar spacings (S) selected to align with the simulations presented in the paper of M.A. Ahamad *et al.*[18]. They predict, using simulations, that specific periodicities of 915nm, 1095nm, 1500nm, and 2315nm ensure the coherent superposition of Mie-scattering resonances within the SiC pillar lattice, enhancing light extraction from embedded color centers. In this work, the periodicity of the arrays is comprised between 730nm and 1450nm, depending on the pillars' diameter and spacing. We also chose a spacing of 5µm for a reference array with no resonances expected due to the large distance between the pillars. However, the conical shape of the chromium masks (FIG.3), combined with lateral etching during the fabrication process, contributes to a reduction in the pillar diameter (Supplementary Materials), which is more pronounced for arrays with larger pillar spacings (945nm and 5µm). This lateral etching, with little impact during SiC power device processing, is significant in nanostructure fabrication and leads to the so-called bowing phenomenon[15,28]. Bowing refers to the lateral etching or undercutting of the pillars' sidewalls, resulting in a curved or bowed profile rather than straight vertical sidewalls. These modifications in the pillars' geometry and diameter can

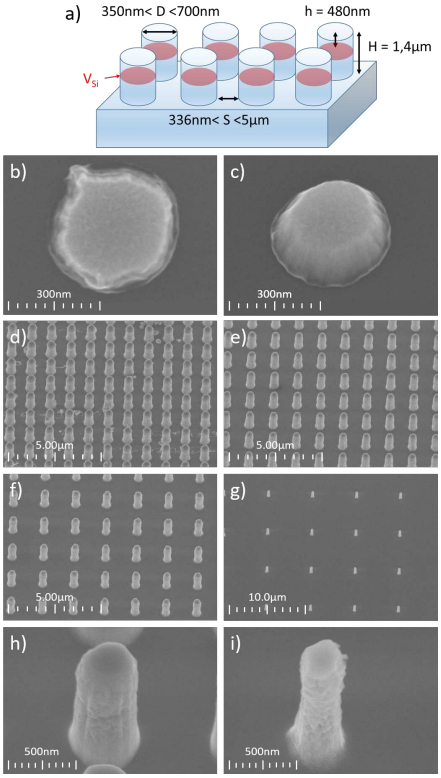

FIG. 3. Scheme of the nanopillar arrays (a) and SEM images with no tilt (b) and a 30° tilt (c) of the Cr-masks for a pillar diameter of 450nm and a spacing of 5µm. SEM images of the nanopillar arrays are also shown for a pillar diameter of 700nm and a spacing of 336nm (d), 538nm (e), 946nm (f), and 5µm (g). Images (h) and (i) are the respective zoom of images (d) and (g).

alter the distribution of the resonant optical modes within the nanostructures, potentially interfering with the light collection efficiency of the silicon vacancies. On the bright side, no evidence of micro-masking or trenching was observed, thanks to the addition of the Si layer, which enhances the volatility of reaction by-products during plasma etching[26]. Trenching caused by ion scattering, over-etching, or charge buildup manifests as deep, narrow grooves ("trenches") at the base or sidewalls of etched features during anisotropic plasma etching[7,29].

Cathodoluminescence (CL) is then used to observe the luminescence of the silicon vacancies in the fabricated nanostructures. This technique can be considered an alternative to photoluminescence (PL) by generating electron-hole recombination through electron beam excitation rather than laser excitation[30,31]. Compared to PL, CL measurements offer a better spatial resolution due to the narrow diameter of the electron beam (about 1.5nm), making it a method adapted for analyzing structures of small dimensions, as the ones realized in this study. Moreover, the high energy of the e-beam (15 keV) enables the excitation of defects located deeper in the material, allowing the easier detection of the silicon vacancies formed approximately 500nm below the samples' surface (FIG.1). However, the high energy of the electrons also results in broadband excitation of the material and its defects (from UV to IR), preventing the excitation of specific transitions as in PL. So, to ensure that the signal observed is associated with the luminescence of the silicon vacancies in 4H-SiC, we realized CL measurements at low temperature (80K) to be able to distinguish the zero phonon lines of the V_{Si} defect from its phonon sidebands. This study performs CL measurements using a SPARC system (Delmic) integrated with a JEOL JSM-7900F SEM. The analysis temperature is maintained at 80K by a liquid nitrogen circulation system (80K Cryo-module, Kammrath and Weiss GmbH, Schwerte, Germany). A diffraction grating of 302 lines/mm with a central wavelength of 500nm is used for spectral analysis, and the SEM is operated at an acceleration voltage of 15kV with a beam current of 1nA. The CL system's spectral detection range extends to 1000nm, allowing detailed analysis of the emitted light from the silicon vacancies.

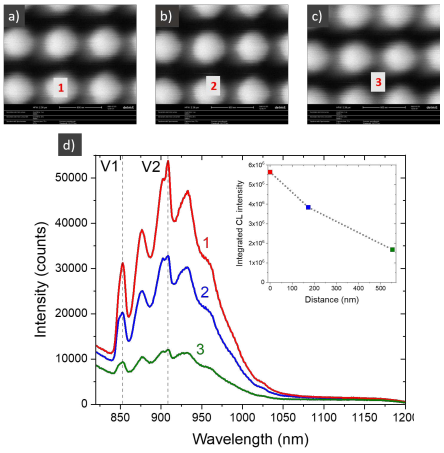

FIG. 4. Cathodoluminescence mapping under electron scanning of an array with a pillar diameter of 500nm and a spacing of 336nm (a-c). The CL spectra (d) are measured at positions 1 to 3. The inset represents the integrated intensity of the CL spectra as a function of the e-beam position during measurements. The e-beam position is expressed as a distance from the nanopillar center.

Using the CASINO software[32,33], we can visualize the electrons' distribution within SiC by Monte Carlo simulations (Supplementary Materials). We calculated an electron penetration depth of approximately 1.14µm. The lateral dispersion of electrons at the depth where most of the V_{Si} defects are located (about 500nm) forms a disk with a diameter of

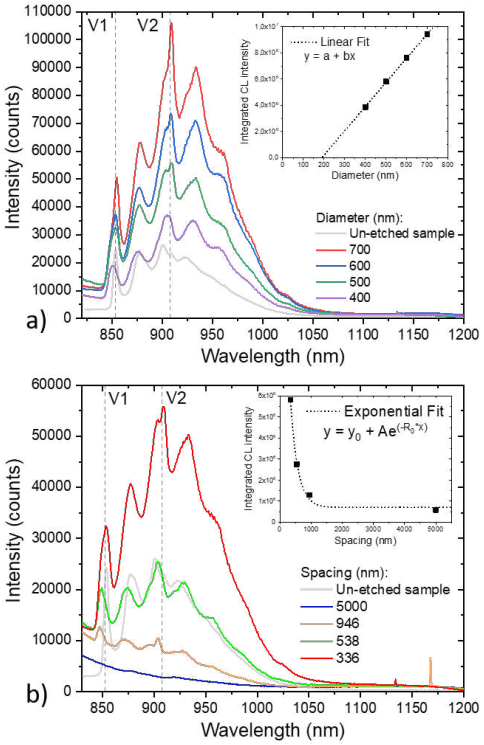

FIG. 5. CL spectra of silicon vacancies for different spacings (a) and diameters (b). The spacing is fixed at 336nm for the graphic (a), and the diameter is fixed at 500nm for the graphic (b). Insets represent the evolution of the calculated area under the CL curves as a function of the pillar's spacing (a) or diameter (b).

approximately 600nm. Since our nanopillars are 1.4 µm tall, the electrons remain confined within the nanostructures and do not significantly scatter into the substrate. Moreover, for a depth of 500nm, the electrons' dispersion is the same order of magnitude as the pillar diameters, so most of the defects within the nanostructures can be effectively irradiated even if the e-beam diameter at the sample's surface is narrow (about 1.5nm). Because CL measurements probe a localized volume of the sample, the intensity of collected light from the V_{Si} defects varies depending on the area analyzed. Mapping of an array with a theoretical pillar diameter of 500nm and a pillar spacing of 336nm (FIG.4) shows that most of the collected light (bright areas in the images) comes from the nanopillars, where the silicon vacancies are localized. The CL spectra show the typical luminescence of V_{Si} defects around the 900nm wavelength[34], confirming their presence within the SiC nanopillars. In 4H-SiC, the silicon vacancies can occupy either cubic (k) or hexagonal (h) sites of the lattice[35], resulting in two zero-phonon lines (ZPLs), called V1 (h) and V2 (k), observed at 850 and 908nm, respectively. The wavelengths of the observed ZPLs are slightly blue-shifted compared to the expected values (862nm for V1 and 917nm for V2)[36], probably due to the local strains introduced into the crystal after ion implantation. Despite the low analysis temperature (80K), phonon sidebands[37,38] are still present in the CL spectra because we are not close enough to absolute zero to fully suppress them. However, the signals of the ZPLs (V1 and V2) remain strong enough to be identified.

We also observe that the CL intensity is highest at the center of the nanopillars (FIG.4). This is because the incident electron beam excites more silicon vacancies when positioned at the pillar center, where the excitation volume overlaps most of the defect-rich region. Unexpectedly, a CL signal is detected in the etched area between the pillars, despite the lack of defects in this region. However, even if lateral electron scattering in SiC allows some interaction between the incident electrons and the nearby pillars, the excitation volume should be well below the V_{Si}-rich region, localized near the top of the pillars. Instead of direct excitation, the CL signal collected in the etched area is more likely due to an optical redistribution of light emitted by the silicon vacancies within the nanopillars. According to the simulations of Ahamad *et al.*[18], the coherent superposition of Mie scattering resonances within the periodic pillar array can lead to this light redistribution for specific array periodicities. Further supporting this hypothesis, we observe a similar CL signal in the etched areas for a pillar spacing of 538 nm (see Supplementary Materials), where Mie resonances are also expected. However, no detectable CL signal is observed in the etched areas for a larger pillar spacing of 5 µm, where no such resonances are predicted.

For the following CL analyses, the electron beam is focused at the center of the pillars to ensure measurement repeatability. As shown in FIG.5.a, the CL intensity from the V_{Si} defects increases linearly with pillar diameter for a given pillar spacing. This behavior can be attributed to the fact that the total number of silicon vacancies scales proportionally with the cross-sectional area of the nanopillars. Unlike previous simulations and experimental studies reported in the literature[16,22], no specific pillar diameter exhibits maximum luminescence for these defects, indicating that in our case, light emission efficiency is mainly governed by defect concentration and excitation volume of electrons.

However, we observe an exponential variation of CL intensity when the spacing decreases (FIG.5.b), with a strong enhancement of light collection for a small pillar spacing. Indeed, for a spacing of 336nm, the CL intensity is enhanced by a factor of two to four compared to the reference sample, depending on the nanopillar diameter. In contrast to Ahamad *et al.*[18], we do not observe distinct maxima in luminescence at specific periodicities corresponding to the coherent superposition of Mie scattering modes. This could be due to bowing and lateral etching that occur during fabrication, which modify the array pitch and pillar geometry, preventing us from reaching the precise geometrical condi-

tions required for these coherent resonances. The exponential increase in CL intensity that we observe can instead be attributed to a general increase in interactions between the Mie-scattering modes of individual pillars as the spacing decreases, resulting in stronger reflectance and enhanced light extraction from the nanopillars[39]. It is also possible that the small inter-pillar spacing can lead to near-field coupling, promoting the formation of low-quality-factor (low-Q) leaky modes such as guided-mode resonances[40], which could also contribute to the enhanced CL signal. Furthermore, in contrast to previous experimental studies that characterized arrays with a periodicity of a few micrometers,[16,22], we observe a lower light collection efficiency than the unprocessed reference sample for larger pillar spacings. This effect is particularly pronounced at a spacing of 5µm, where the CL signal is extremely weak (see Supplementary Materials). This discrepancy may arise from differences in defect distribution. Indeed, in prior studies, V_{Si} defects were intentionally introduced within the etched surface, whereas in our fabrication process, SiC etching was realized after ion implantation. As a result, silicon vacancies were generated exclusively within the pillars, with none present in the etched surface, apart from the intrinsic defects of the 4H-SiC substrate.

This study highlights the potential of silicon carbide (SiC) nanopillar arrays as scalable and efficient platforms for enhancing light collection from color centers such as silicon vacancies in 4H-SiC. By combining color centers' generation and nanopillar fabrication, we demonstrate the compatibility of SiC with photonic structures designed for quantum applications. Due to the high applicability of ion implantation and plasma etching, this technological platform could also be adapted to integrate different color centers in other polytypes of SiC, such as 3C or 6H-SiC, increasing the panel of single photon sources available. While the results confirm the influence of pillar geometry and array periodicity on light collection efficiency, further work is needed to understand better the underlying physical principles. Experiments with isolated single V_{Si} defects are essential to confirm single-photon emission properties and assess the platform's potential for quantum technologies. Exploring arrays with even smaller spacings near 336nm would also help elucidate how the CL signal evolves as the pillars approach each other, potentially unlocking more regimes of photonic interaction. Finally, improvements in fabrication processes to minimize SiC lateral etching and preserve pillar integrity could further enhance device performance. In conclusion, this work establishes a foundation for integrating quantum defects in SiC with photonic structures, paving the way for applications in quantum sensing, single-photon sources, and scalable quantum photonic devices. Future studies addressing the above challenges will bring us closer to realizing the full potential of SiC for quantum technologies.

The Supplementary Materials details the fabrication steps of the 4H-SiC nanopillar arrays and the evolution of lateral etching with pillar diameters and spacings. Information about the electrons' excitation volume in cathodoluminescence measurements is also provided, as well as more details on CL characterization of some arrays.

Samples were implanted in the IP2I institute at Lyon in France. The authors acknowledge the use of resources from the Nanomat platform, part of the RENATECH network, supported by the Ministère de l'Enseignement Supérieur et de la Recherche, the Région Grand Est, and FEDER funds from the European Community. This work was made within the context of the graduate school NANO-PHOT - ANR-18-EURE-0013.

The authors have no conflicts of interest to disclose.

The authors contributions are specified below. **E. Vuillermet**: Conceptualization; Formal analysis; Investigation; Methodology; Validation; Writing – original draft; Writing – review and editing. **S. Kostcheev**: Investigation; Methodology. **N. Bercu**: Investigation; Methodology. **M. Lazar**: Conceptualization; Funding acquisition; Supervision; Validation; Writing – review and editing.

The data that support the findings of this study are available from the corresponding author upon reasonable request.

REFERENCES

[1]X. She, A. Q. Huang, O. Lucia, and B. Ozpineci, "Review of silicon carbide power devices and their applications," IEEE Transactions on Industrial Electronics **64**, 8193–8205 (2017).
[2]H. Matsunami, "Fundamental research on semiconductor sic and its applications to power electronics," Proceedings of the Japan Academy, Series B **96**, 235–254 (2020).
[3]S. Castelletto and A. Boretti, "Silicon carbide color centers for quantum applications," Journal of Physics: Photonics **2**, 022001 (2020).
[4]A. S. Al Atem, *Ingénierie des centres colorés dans SiC pour la photonique et la solotronique*, Ph.D. thesis, Université de Lyon (2018).
[5]T. Kimoto, "Bulk and epitaxial growth of silicon carbide," Progress in Crystal Growth and Characterization of Materials **62**, 329–351 (2016).
[6]D. Chaussende and N. Ohtani, "Silicon carbide," Single crystals of electronic materials , 129–179 (2019).
[7]K. Racka-Szmidt, B. Stonio, J. Żelazko, M. Filipiak, and M. Sochacki, "A review: Inductively coupled plasma reactive ion etching of silicon carbide," Materials **15**, 123 (2021).
[8]V. A. Norman, S. Majety, Z. Wang, W. H. Casey, N. Curro, and M. Radulaski, "Novel color center platforms enabling fundamental scientific discovery," InfoMat **3**, 869–890 (2021).
[9]M. E. Bathen and L. Vines, "Manipulating single-photon emission from point defects in diamond and silicon carbide," Advanced Quantum Technologies **4**, 2100003 (2021).
[10]S. Castelletto, C. Lew, W.-X. Lin, and J.-S. Xu, "Quantum systems in silicon carbide for sensing applications," Reports on Progress in Physics (2023).
[11]K. Khazen and H. J. von Bardeleben, "Nv-centers in sic: A solution for quantum computing technology?" Frontiers in Quantum Science and Technology **2**, 1115039 (2023).
[12]Y. Yamazaki, Y. Chiba, T. Makino, S.-I. Sato, N. Yamada, T. Satoh, Y. Hijikata, K. Kojima, S.-Y. Lee, and T. Ohshima, "Electrically controllable position-controlled color centers created in sic pn junction diode by proton beam writing," Journal of Materials Research **33**, 3355–3361 (2018).
[13]S. Rao, E. D. Mallemace, G. Faggio, M. Iodice, G. Messina, and F. G. Della Corte, "Experimental characterization of the thermo-optic coefficient vs. temperature for 4h-sic and gan semiconductors at the wavelength of 632 nm," Scientific Reports **13**, 10205 (2023).
[14]D. M. Lukin, M. A. Guidry, J. Yang, M. Ghezellou, S. Deb Mishra, H. Abe, T. Ohshima, J. Ul-Hassan, and J. Vučković, "Two-emitter multimode cavity

quantum electrodynamics in thin-film silicon carbide photonics," Physical Review X **13**, 011005 (2023).
[15]D. O. Bracher and E. L. Hu, "Fabrication of high-q nanobeam photonic crystals in epitaxially grown 4h-sic," Nano letters **15**, 6202–6207 (2015).
[16]M. Radulaski, M. Widmann, M. Niethammer, J. L. Zhang, S.-Y. Lee, T. Rendler, K. G. Lagoudakis, N. T. Son, E. Janzen, T. Ohshima, *et al.*, "Scalable quantum photonics with single color centers in silicon carbide," Nano letters **17**, 1782–1786 (2017).
[17]M. Salomoni, R. Pots, E. Auffray, and P. Lecoq, "Enhancing light extraction of inorganic scintillators using photonic crystals," Crystals **8**, 78 (2018).
[18]M. A. Ahamad, N. Ahmed, S. Castelletto, and F. A. Inam, "Silicon carbide pillar lattice for controlling the spontaneous emission of embedded color centers," Journal of Lightwave Technology (2023).
[19]F. A. Inam and S. Castelletto, "Understanding the photonics of single color-center emission in a high-indexed nano-pillar," Journal of Applied Physics **130** (2021).
[20]M. Widmann, S.-Y. Lee, T. Rendler, N. T. Son, H. Fedder, S. Paik, L.-P. Yang, N. Zhao, S. Yang, I. Booker, *et al.*, "Coherent control of single spins in silicon carbide at room temperature," Nature materials **14**, 164–168 (2015).
[21]D. Simin, H. Kraus, A. Sperlich, T. Ohshima, G. Astakhov, and V. Dyakonov, "Locking of electron spin coherence above 20 ms in natural silicon carbide," Physical Review B **95**, 161201 (2017).
[22]S. Castelletto, A. S. Al Atem, F. A. Inam, H. J. von Bardeleben, S. Hameau, A. F. Almutairi, G. Guillot, S.-i. Sato, A. Boretti, and J. M. Bluet, "Deterministic placement of ultra-bright near-infrared color centers in arrays of silicon carbide micropillars," Beilstein Journal of Nanotechnology **10**, 2383–2395 (2019).
[23]V. Shulga, "Simulation of ion beam sputtering with oksana and srim: A comparative study," Vacuum **230**, 113644 (2024).
[24]I. Strašík and M. Pavlovič, "Improvements to the srim simulations," Radiation Effects & Defects in Solids **164**, 470–476 (2009).
[25]L. Voss, K. Ip, S. Pearton, R. Shul, M. Overberg, A. Baca, C. Sanchez, J. Stevens, M. Martinez, M. Armendariz, *et al.*, "Sic via fabrication for wide-band-gap high electron mobility transistor/microwave monolithic integrated circuit devices," Journal of Vacuum Science & Technology B: Microelectronics and Nanometer Structures Processing, Measurement, and Phenomena **26**, 487–494 (2008).
[26]M. Lazar, F. Enoch, F. Laariedh, D. Planson, and P. Brosselard, "Influence of the masking material and geometry on the 4h-sic rie etched surface state," in *Materials Science Forum*, Vol. 679 (Trans Tech Publ, 2011) pp. 477–480.
[27]M. Lazar, H. Vang, P. Brosselard, C. Raynaud, P. Cremillieu, J.-L. Leclercq, A. Descamps, S. Scharnholz, and D. Planson, "Deep sic etching with rie," Superlattices and microstructures **40**, 388–392 (2006).
[28]K. Zekentes, J. Pezoldt, and V. Veliadis, "Plasma etching of silicon carbide," Mater. Res. Found **69**, 175–232 (2020).
[29]F. Simescu, D. Coiffard, M. Lazar, P. Brosselard, D. Planson, *et al.*, "Study of trenching formation during sf6/o2 reactive ion etching of 4h-sic," Journal of optoelectronics and advanced materials **12**, 766–769 (2010).
[30]B. Sieber, "Cathodoluminescence-principes physiques et systèmes de détection," Editions TI| Techniques de l'Ingénieur (2012).
[31]A. Kakanakova-Georgieva, R. Yakimova, A. Henry, M. K. Linnarsson, M. Syväjärvi, and E. Janzén, "Cathodoluminescence identification of donor–acceptor related emissions in as-grown 4h–sic layers," Journal of applied physics **91**, 2890–2895 (2002).
[32]H. Demers, N. Poirier-Demers, A. R. Couture, D. Joly, M. Guilmain, N. de Jonge, and D. Drouin, "Three-dimensional electron microscopy simulation with the casino monte carlo software," Scanning **33**, 135–146 (2011).
[33]D. Drouin, A. Couture, and R. Gauvin, "Casino v2. 0: An advance simulation tool for scanning electron microscope users," Microscopy and Microanalysis **7**, 684–685 (2001).
[34]E. Vuillermet, N. Bercu, F. Etienne, and M. Lazar, "Cathodoluminescence characterization of point defects generated through ion implantations in 4h-sic," Coatings **13**, 992 (2023).
[35]F. A. Inam and S. Castelletto, "Metal-dielectric nanopillar antenna-resonators for efficient collected photon rate from silicon carbide color centers," Nanomaterials **13**, 195 (2023).
[36]M. Wagner, B. Magnusson, W. Chen, E. Janzén, E. Sörman, C. Hallin, and J. Lindström, "Electronic structure of the neutral silicon vacancy in 4 h and 6 h sic," Physical Review B **62**, 16555 (2000).
[37]T. Sun, Z. Xu, J. Wu, Y. Fan, F. Ren, Y. Song, L. Yang, and P. Tan, "Di-vacancy and silicon vacancy color centers in 4h-sic fabricated by hydrogen and dual ions implantation and annealing," Ceramics International **49**, 7452–7465 (2023).
[38]J. Wang, Y. Zhou, X. Zhang, F. Liu, Y. Li, K. Li, Z. Liu, G. Wang, and W. Gao, "Efficient generation of an array of single silicon-vacancy defects in silicon carbide," Physical Review Applied **7**, 064021 (2017).
[39]F. J. Bezares, J. P. Long, O. J. Glembocki, J. Guo, R. W. Rendell, R. Kasica, L. Shirey, J. C. Owrutsky, and J. D. Caldwell, "Mie resonance-enhanced light absorption in periodic silicon nanopillar arrays," Optics Express **21**, 27587–27601 (2013).
[40]G. Quaranta, G. Basset, O. J. Martin, and B. Gallinet, "Recent advances in resonant waveguide gratings," Laser & Photonics Reviews **12**, 1800017 (2018).